

# A Missense Mutation of the Gene Encoding Voltage-Dependent Sodium Channel (Na<sub>v</sub>1.1) Confers Susceptibility to Febrile Seizures in Rats

Tomoji Mashimo,<sup>1</sup> Iori Ohmori,<sup>2</sup> Mamoru Ouchida,<sup>3</sup> Yukihiro Ohno,<sup>4</sup> Toshiko Tsurumi,<sup>1</sup> Takafumi Miki,<sup>5</sup> Minoru Wakamori,<sup>6</sup> Shizuka Ishihara,<sup>4</sup> Takashi Yoshida,<sup>6</sup> Akiko Takizawa,<sup>1</sup> Megumi Kato,<sup>7</sup> Masumi Hirabayashi,<sup>7</sup> Masashi Sasa,<sup>8</sup> Yasuo Mori,<sup>5</sup> and Tadao Serikawa<sup>1</sup>

<sup>1</sup>Institute of Laboratory Animals, Graduate School of Medicine, Kyoto University, Kyoto 606-8501, Japan, Departments of <sup>2</sup>Physiology and <sup>3</sup>Molecular Genetics, Graduate School of Medicine, Dentistry, and Pharmaceutical Sciences, Okayama University, Okayama 700-8558, Japan, <sup>4</sup>Laboratory of Pharmacology, Osaka University of Pharmaceutical Sciences, Takatsuki, Osaka 569-1094, Japan, <sup>5</sup>Laboratory of Molecular Biology, Department of Synthetic Chemistry and Biological Chemistry Graduate School of Engineering, Kyoto University, Kyoto 615-8501, Japan, <sup>6</sup>Department of Oral Biology, Graduate School of Dentistry, Tohoku University, Sendai 980-8575, Japan, <sup>7</sup>Center for Genetic Analysis of Behavior, National Institute for Physiological Sciences, Okazaki 444-8587, Japan, and <sup>8</sup>Nagisa Hospital, Hirakata, Osaka 573-1183, Japan

Although febrile seizures (FSs) are the most common convulsive syndrome in infants and childhood, the etiology of FSs has remained unclarified. Several missense mutations of the Na<sub>v</sub>1.1 channel (SCN1A), which alter channel properties, have been reported in a familial syndrome of GEFS+ (generalized epilepsy with febrile seizures plus). Here, we generated *Scn1a*-targeted rats carrying a missense mutation (N1417H) in the third pore region of the sodium channel by gene-driven ENU (*N*-ethyl-*N*-nitrosourea) mutagenesis. Despite their normal appearance under ordinary circumstances, *Scn1a* mutant rats exhibited remarkably high susceptibility to hyperthermia-induced seizures, which involve generalized clonic and/or tonic–clonic convulsions with paroxysmal epileptiform discharges. Whole-cell patch-clamp recordings from HEK cells expressing N1417H mutant channels and from hippocampal GABAergic interneurons of N1417H mutant rats revealed a significant shift of the inactivation curve in the hyperpolarizing direction. In addition, clamp recordings clearly showed the reduction in action potential amplitude in the hippocampal interneurons of these rats. These findings suggest that a missense mutation (N1417H) of the Na<sub>v</sub>1.1 channel confers susceptibility to FS and the impaired biophysical properties of inhibitory GABAergic neurons underlie one of the mechanisms of FS.

## Introduction

Febrile seizures (FSs) are the most common type of convulsive events in childhood between 6 months and 6 years of age, affecting 2–5% of children worldwide. Most FSs are apparently benign (categorized as simple), but one-third are complex with a prolonged duration (>15 min) and are associated with a risk of subsequent epilepsy. Essentially, any illness that leads to an increase in body temperature, such as upper respiratory infection, pneumonia, and influenza, and even bathing, can lead to FS (Fukuda et al., 1997). Several familial studies and twin studies have indicated that genetic predisposition may contribute significantly to the etiology of FS, and recent genetic studies have

shown that at least nine loci are responsible for FS (Nakayama, 2009).

Voltage-gated sodium channels are critical for the initiation and propagation of action potentials in neurons. Mutations in the human Na<sub>v</sub>1.1 channel gene SCN1A have been reported in >200 cases, ranging in severity from the comparatively mild disorder of generalized epilepsy with febrile seizures plus (GEFS+) to the epileptic encephalopathy of severe myoclonic epilepsy in infancy (SMEI). In GEFS+, FS persists beyond the age of 6 and may be accompanied by various other seizure types, including tonic–clonic, absence, and myoclonic seizures (Scheffer and Berkovic, 1997). SMEI, also known as Dravet's syndrome, is a severe epileptic encephalopathy, characterized by onset of FS by age 1 and the emergence between ages 1 and 4 of other seizure types, including myoclonic, focal, absence, and atonic seizures, along with developmental decline (Dravet et al., 2005). All SCN1A mutations responsible for GEFS+ have been found to be missense mutations, whereas one-half of the mutations in SMEI are truncated and presumably loss of function, and the remaining one-half are missense mutations (Meisler and Kearney, 2005; Mulley et al., 2005; Lossin, 2009).

Animal models of FS have contributed to fundamental understanding of the underlying mechanisms of FS (Holtzman et al.,

Received July 8, 2009; revised March 2, 2010; accepted March 10, 2010.

This work was supported in part by a research grant from the Japan Epilepsy Research Foundation; Ministry of Education, Culture, Sports, Science and Technology Grant-in-Aid for Scientific Research 16200029; and Industrial Technology Research Grant Program in 2008 from New Energy and the Industrial Technology Development Organization of Japan. We thank T. Kuramoto and B. Voigt for critical discussion and movie preparation, and F. Tagami, Y. Kunihiro, S. Tokuda, N. Sofue, and S. Nakanishi for experimental assistance.

Correspondence should be addressed to Tomoji Mashimo, Institute of Laboratory Animals, Kyoto University Graduate School of Medicine, Yoshidakonoe-cho, Sakyo-ku, Kyoto 606-8501, Japan. E-mail: tmashimo@anim.med.kyoto-u.ac.jp.

DOI:10.1523/JNEUROSCI.3360-09.2010

Copyright © 2010 the authors 0270-6474/10/305744-10\$15.00/0

1981). In a well established model, exposing rat pups to hyperthermia provokes seizures with elevating body temperature to a level comparable with human fever (Chen et al., 1999; Schuchmann et al., 2006). Mice heterozygous for the knock-out allele at the *Scn1a* locus have been recently reported as a potential animal model of SMEI (Yu et al., 2006; Ogiwara et al., 2007): these mice mainly develop epileptic seizures, whereas homozygous mice show ataxia and die on postnatal day 15. Very recently, hyperthermia stimuli of the heterozygous mice demonstrated seizure susceptibility before the spontaneous seizure developed (Oakley et al., 2009). Although these observations can explain the epileptic phenotype of SMEI, the relationship between sodium channel functions and the onset of FS is still poorly understood. It is likely that the best animal models for FS would not result from a null allele of the *Scn1a*, but rather from an allele with a missense mutation.

In this study, using gene-driven *N*-ethyl-*N*-nitrosourea (ENU) mutagenesis, we generated *Scn1a*-targeted rats carrying a missense mutation (N1417H) in the third pore region of the sodium channel. *Scn1a* mutant rats exhibited markedly high susceptibility to experimental FS, thus designated as hyperthermia-induced seizure-susceptible (Hiss) rats. The N1417H mutation of *Scn1a* resulted in abnormal inactivation of Na<sub>v</sub>1.1 channels at hyperpolarized membrane potentials. This mutation in the rat allows additional investigations to understand the etiology of FS and/or associated epilepsies.

## Materials and Methods

All animal care and experiments conformed to the Guidelines for Animal Experiments at Kyoto University and were approved by the Animal Research Committee of Kyoto University.

**ENU mutagenesis in rats.** ENU mutagenesis procedures in rats were previously described (Mashimo et al., 2008). Briefly, we administered two doses of 40 mg/kg ENU by intraperitoneal injection to F344/NSlc male rats at 9 and 10 weeks of age. Ten weeks after the second ENU treatment, males were mated with F344/NSlc females to generate 1735 G<sub>1</sub> male offspring, whose genomic DNA and sperm were cryopreserved in the Kyoto University Rat Mutant Archive (KURMA) (Mashimo et al., 2008). The sperm archive KURMA has been deposited in the National Bio Resource Project for the Rat in Japan ([www.anim.med.kyoto-u.ac.jp/nbr](http://www.anim.med.kyoto-u.ac.jp/nbr)) and is open to any interested researcher worldwide. For sperm cryopreservation, a clump of spermatozoa were taken from the caudal epididymides of 10-week-old rats and dispersed in 1 ml of mR1ECM medium (Hirabayashi et al., 2002). The sperm suspension was then sonicated for 10 s with an ultrasonic cell disruptor (UR-20P; Tomy Seiko) and transferred into 1.0 ml microtubes (Nalge Nunc International). The sperm tubes were frozen in liquid nitrogen vapor and finally stored in liquid nitrogen.

Screening protocols with MuT-POWER on the KURMA were described previously (Mashimo et al., 2008). Eight independent G<sub>1</sub> DNA samples were pooled for subsequent PCRs. Primers were designed to amplify the exonic region of the rat *Scn1a* gene from ~50 bp flanking each intron (supplemental Table 1, available at [www.jneurosci.org](http://www.jneurosci.org) as supplemental material). PCRs were performed in a total volume of 15  $\mu$ l under the following conditions: 94°C for 3 min for 1 cycle, 94°C for 30 s, 60°C for 30 s, and 72°C for 1 min for 35 cycles. The final reaction conditions were 100 ng of genomic DNA, 200  $\mu$ M each dNTP, 1.0 mM MgCl<sub>2</sub>, 0.66  $\mu$ M each primer, and 0.4 U of TaqDNA polymerase (Invitrogen). The Mu transposition reactions were previously described (Yanagihara and Mizuuchi, 2002). The Mu transpososome mixture was prepared by mixing 300 nM MuA transposase, 100 nM labeled Mu-end DNA, and 25 mM HEPES, pH 7.6, 15% (v/v) glycerol, 15% DMSO, 10 mM 3-[(3-cholamidopropyl)dimethylammonio]-1-propanesulfonate (CHAPS), and 156 mM NaCl. Reactions were performed at 30°C for 1 h. The mixture was then split and mixed with PCR products and MgCl<sub>2</sub> activation buffer. The final Mu transposition reaction mixture contained 33 nM

labeled Mu-end DNA, 100 nM MuA transposase, PCR products, 25 mM HEPES, pH 7.6, 15% (v/v) glycerol, 10% DMSO, 10 mM CHAPS, 10 mM MgCl<sub>2</sub>, and 300 mM NaCl. Reactions were performed at 20°C for 5 min. The reaction mixture was then purified by CleanSEQ (Beckman Coulter) to remove dye-labeled oligos, followed by automatic electrophoresis on a 16-capillary 3100 DNA Sequencer (Applied Biosystems). When positive peaks were detected in the eight pooled samples by MuT-POWER screening, individual sequences of the eight independent samples were determined. The sequencing reactions were performed with BigDye terminator, version 3.1, cycle sequencing mix, followed by the standard protocol for the Applied Biosystems 3100 DNA Sequencer.

In the intracytoplasmic sperm injection (ICSI) procedure, sperm heads were injected into denuded oocytes at ambient temperature (23  $\pm$  2°C) using a piezo impact-driving unit (PMM-150FU; Prime Tech) with a pulse controller (PMAS-CT150; Prime Tech). ICSI oocytes were cultured in 60  $\mu$ l microdrops of mR1ECM medium at 37°C under mineral oil in 5% CO<sub>2</sub> in air. All nondegenerating one-cell oocytes and evenly cleaved two-cell oocytes at 23–25 h after ICSI were transferred into the oviductal ampullae of recipient Wistar/ST rats that had been previously mated with vasectomized males. Embryo transfers were performed on the day when the vaginal plug was detected (defined as day 1).

To eliminate mutations that might have been generated by ENU in other chromosomal regions of the *Scn1a* locus, more than five backcross generations were performed against the F344/NSlc inbred background. Heterozygous carriers were then intercrossed to produce homozygous individuals. The mean mutation frequency was ~1 in 4.0 million base pairs (Mashimo et al., 2008). Although the chance for the occurrence of a very tightly linked mutation with a phenotypic effect is very small, this possibility should be taken into account for the experimental design and interpretation of the results. We compared littermates to validate the effect of the observed mutation and to minimize the possibility of the before-mentioned circumstances.

**Pentylentetrazol- and hyperthermia-induced seizures.** Pentylentetrazol (PTZ) (Sigma-Aldrich) dissolved in saline was injected into the tail vein at three doses (10, 20, and 30 mg/kg) to 10- to 12-week-old male rats. The epileptic (ED<sub>50</sub>) and lethal (LD<sub>50</sub>) dose of PTZ, which induced seizures and associated death, respectively, in 50% of animals, was calculated by probit analysis.

Although exposing rat pups to a stream of hot air from a hair dryer has been a widely used model of experimental febrile seizures, we used hot water bathing since it can induce seizures in rats for a wider range of ages (1–10 weeks). Hot water-induced seizures were described by Klauenberg and Sparber (1984). A 30  $\times$  60  $\times$  60 tank contained 15-cm-deep 45°C water, whose temperature was controlled by a heater. The rats were placed in hot water for a maximum of 5 min or until a seizure occurred. The rectal temperature of rats was measured before and immediately after onset of the seizure with a probe inserted into the rectum (BAT-12; Physitemp). Diazepam (Wako) dissolved in 40% polyethyleneglycol solution (0.5 mg/kg) was administered intraperitoneally to the animals 30 min before the experiment.

For EEG recording, rats of 4 weeks of age were anesthetized with an intraperitoneal injection of pentobarbital (40 mg/kg, i.p.). With the animal's head fixed in a stereotaxic instrument (David Kopf), screw electrodes were placed on the right or left frontal and occipital cortex. A reference electrode was placed on the frontal cranium. The electrodes were then connected to a miniature plug and fixed to the skull with dental cement. After a 1 week recovery period, animals with implanted electrodes were subjected to the hyperthermia-induced seizure (HIS) experiments described above. Cortical EEGs were recorded, under free-moving conditions, with an amplifier (MEG-6108; Nihon Kohden) and a recorder (RTA-1100; Nihon Kohden), and the signals were stored in a computer (ML845; PowerLab) for later analysis. Behavioral changes were simultaneously observed.

**Expression analysis of *Scn1a*.** Whole brains were isolated from F344/NSlc and Hiss rats at postnatal ages 1, 2, 3, 5, and 10 weeks ( $n = 3$  each). Total RNA samples were extracted by Isogen reagent (Nippon Gene). First-strand cDNA was synthesized from 5  $\mu$ g of DNase-treated total RNA using oligo-dT<sub>12-18</sub> primer and SuperScript II reverse transcriptase (Invitrogen). Quantitative PCR was performed using SYBR Premix Ex Taq polymerase and a Thermal Cycler Dice Real-Time System TP800 (Takara). The following

primers were used to specifically amplify respective genes: rat *Scn1a* gene, 5'-TTGCTTTGGAATCAGCATCTC-3' and 5'-GAGGTGCCTATGGTCTGCTCTGTA-3'; rat *Scn3a* gene, 5'-CGATGCAATTCACCCCTGG-AAG-3' and 5'-GTGGCGACGCTGAAGTTCTC-3'. The cycling conditions comprised 10 s polymerase activation at 95°C and 30 cycles at 95°C for 5 s and 60°C for 30 s. The data acquisition step was performed at 60°C, and final melting curve analysis was used to ensure amplification of a single product. This experiment was performed three times independently, and each RNA sample was analyzed at least in duplicate. All relative quantification of gene expression with real-time PCR data was performed using the comparative threshold (Ct) cycle method. The Ct values of target genes were normalized to the levels of GAPDH as an endogenous control at each time point.

Western blotting was performed using the cell lysate from the hippocampus using standard methods. Signals were detected with antibodies against rat Na<sub>v</sub>1.1 (AB5204; Millipore Bioscience Research Reagents) and β-actin (AC-40; Sigma-Aldrich).

**Electrophysiological recordings of heterologously expressed recombinant SCN1A.** Full-length human SCN1A (Na<sub>v</sub>1.1) cDNA was provided by Dr. Al George (Vanderbilt University, Nashville, TN). The N1417H mutation was constructed by PCR-based site-directed mutagenesis. The N1417H fragment was digested with BglII and Sall, and then replaced the corresponding restriction fragment in the pCMVscript-SCN1A wild type (WT). The open reading frame of every construct was completely sequenced before use to exclude polymerase errors and rearrangements. Recombinant SCN1A-WT and N1417H were heterologously coexpressed with human β1 and β2 accessory subunits (generous gifts from Dr. Al George) in human embryonic kidney (HEK)-293 cells. Whole-cell voltage-clamp recordings were performed to characterize the functional properties of WT-SCN1A and N1417H. HEK-293 cells were grown in DMEM supplemented with 10% (v/v) fetal bovine serum (Atlanta Biologicals), 2 mM L-glutamine, and penicillin-streptomycin (50 U/ml and 50 μg/ml, respectively) in a humidified 5% CO<sub>2</sub> atmosphere at 37°C. Expression of SCN1A, β1, and β2 was achieved by transient plasmid transfection using QIAGEN Superfect reagent. Sodium channel currents were recorded from transfected HEK293 cells at room temperature using Axopatch 200B amplifiers (Molecular Devices). Pipette resistance was between 1.3 and 2.0 MΩ. The pipette solution consisted of the following (in mM): 110 CsF, 10 NaF, 20 CsCl, 2 EGTA, 10 HEPES, with a pH of 7.35 and osmolarity of 310 mOsmol/kg. The bath solution consisted of the following (in mM): 145 NaCl, 4 KCl, 1.8 CaCl<sub>2</sub>, 1 MgCl<sub>2</sub>, 10 HEPES, with a pH of 7.35 and osmolarity of 310 mOsmol/kg. Cells were allowed to stabilize for 10 min after establishing the whole-cell configuration before currents were recorded. Whole-cell capacitance and access resistance were determined by integrating capacitive transients in response to voltage steps from -120 to -110 mV filtered at 5 kHz. Series resistance (2 ± 0.1 MΩ) was compensated 87–95% to assure that the command potential was reached within microseconds with a voltage error <3 mV. Leak currents were subtracted using the P/4 procedure. All data were low-pass Bessel filtered at 5 kHz and digitized at 10–50 kHz. Specific voltage-clamp protocols assessing channel activation, steady-state inactivation, and recovery from fast inactivation were used. Representations of all voltage protocols are included as insets in the figures. Persistent current was evaluated during the final 10 ms of a 100 ms depolarization to -10 mV and expressed as a percentage of peak current after digital subtraction of currents recorded in the presence and absence of 10 μM tetrodotoxin (TTX) (Sigma-Aldrich). Results are presented as the mean ± SEM, and statistical comparisons were made in reference to WT-SCN1A using the unpaired Student's *t* test. Data analysis was performed by using Clampfit 8.2 (Molecular Devices) and OriginPro 7.0 (OriginLab) software.

**Whole-cell recording in dissociated hippocampal neurons.** Hippocampal pyramidal cells and bipolar cells were freshly dissociated from 11- to 16-d-old F344/NSlc and Hiss (*Scn1a*<sup>Kyo811/Kyo811</sup>) rats. Coronal slices (350 μm thick) of the hippocampus were prepared using a microslicer (Linear Slice PRO7; Dosaka). After preincubation in Krebs' solution for 40 min at 31°C, the slices were digested: first in Krebs' solution containing 0.017% Pronase (Calbiochem/Novabiochem) for 20 min at 31°C, and then in solution containing 0.017% thermolysin (type X; Sigma-Aldrich) for 20 min at 31°C. The Krebs' solution used for preincubation and digestion contained the following (in mM): 124 NaCl, 5 KCl, 1.2

KH<sub>2</sub>PO<sub>4</sub>, 2.4 CaCl<sub>2</sub>, 1.3 MgSO<sub>4</sub>, 24 NaHCO<sub>3</sub>, and 10 glucose. The solution was continuously oxygenated with 95% O<sub>2</sub> and 5% CO<sub>2</sub>. CA1 regions at the pyramidal layer or at a distance of 50–200 μm from the pyramidal layer were punched out and dissociated mechanically using fine glass pipettes with a tip diameter of 100–200 μm. Dissociated cells settled on tissue culture dishes (Primaria no. 3801; BD Biosciences) within 30 min. Hippocampal bipolar neurons were identified by their bipolar shape.

Electrophysiological measurements were performed on hippocampal pyramidal cells and bipolar cells. Currents were recorded at room temperature (22–25°C) using the whole-cell mode of the patch-clamp technique with an EPC-9 patch-clamp amplifier (HEKA). Patch pipettes were made from borosilicate glass capillaries (1.5 mm outer diameter; Hilgenberg) using a model P-97 Flaming-Brown micropipette puller (Sutter Instrument). Pipette resistance ranged from 2 to 4 MΩ when filled with the pipette solutions described below. Series resistance was electronically compensated to >50%, and both the leakage and remaining capacitance were subtracted by the -P/5 method. Currents were sampled at 100 kHz after low-pass filtering at 10 kHz. Stimulation and data acquisition were performed using the PULSE program (version 7.5; HEKA Elektronik). Sodium currents were recorded in an external solution that contained the following (in mM): 19.1 NaCl, 19.1 TEA-Cl (tetraethylammonium chloride), 0.95 BaCl<sub>2</sub>, 1.90 MgCl<sub>2</sub>, 52.4 CsCl, 0.1 CdCl<sub>2</sub>, 0.95 CaCl<sub>2</sub>, 9.52 HEPES, 117 glucose, pH adjusted to 7.35 with NaOH. The pipette solution contained the following (in mM): 157 N-methyl-D-glucamine (NMDG), 126 HCl, 0.90 NaCl, 3.60 MgCl<sub>2</sub>, 9.01 EGTA, 1.80 ATPNa<sub>2</sub>, 9.01 HEPES, 4.50 creatine-phosphate, pH adjusted to 7.2 with NMDG. Conductance-voltage (*g*-*V*) relationships were calculated from current-voltage (*I*-*V*) relationships according to  $g = I_{Na} / (V - E_{Na})$ , where *I*<sub>Na</sub> represents the peak sodium current measured at potential *V*, and *E*<sub>Na</sub> represents the equilibrium potential. Normalized activation and inactivation curves were fitted to Boltzmann relationships of the following form:  $y = 1 / (1 + \exp[(V_{0.5} - V) / k])$ , where *y* is normalized *g*<sub>Na</sub> or *I*<sub>Na</sub>, *V* is the membrane potential, *V*<sub>0.5</sub> is the voltage of half-maximal activation, or inactivation, and *k* is the slope factor. Inactivation time constants were evaluated by fitting the current decay with single exponential function:  $I = A \times \exp(-t/\tau) + C$ , where *I* is the current, *A* is the current inactivated with time constants *τ*, and *C* is the noninactivating current.

Whole-cell voltage recordings were made at room temperature (22–25°C) using the current-clamp mode with an Axopatch 200B patch-clamp amplifier (Molecular Devices). Hippocampal pyramidal cells and bipolar cells were held at -80 mV, and their firing patterns were recorded in response to sustained depolarizations or hyperpolarizations (duration, 800 ms; increments, ±5 pA) (Yu et al., 2006). The intracellular solution contained the following (in mM): 135 potassium gluconate, 20 KCl, 2 MgCl<sub>2</sub>, 2 ATPNa<sub>2</sub>, 0.3 GTPNa, and 10 HEPES, 0.2 EGTA, pH adjusted to 7.3 with KOH. The extracellular solution contained the following (in mM): 140 NaCl, 5 KCl, 2 CaCl<sub>2</sub>, 1 MgCl<sub>2</sub>, 10 HEPES, and 10 glucose, pH adjusted to 7.4 with NaOH. The input-output relationship, action potential half-width, spike amplitude, and spike decrement were measured. The input-output relationship was defined as the dependence of the number of action potentials generated on the amplitude of current injection. Action potential half-width was defined as the width at half-maximum amplitude of the action potential. Spike decrement was calculated as percentage of last spike amplitude divided by first spike amplitude.

Statistical comparison between F344/NSlc and Hiss rats was performed by Student's *t* test (\**p* < 0.05; \*\**p* < 0.01; \*\*\**p* < 0.001).

## Results

### Targeted mutations in the rat *Scn1a*

To generate a rat model carrying a mutation in the *Scn1a*, we used the chemical mutagen ENU and our recently developed strategy, combining a high-throughput screening assay making use of the Mu-transposition reaction (MuT-POWER) and ICSI to recover rare heterozygous mutations from our frozen sperm repository (Mashimo et al., 2008). Screening of 1735 G<sub>1</sub> samples by MuT-

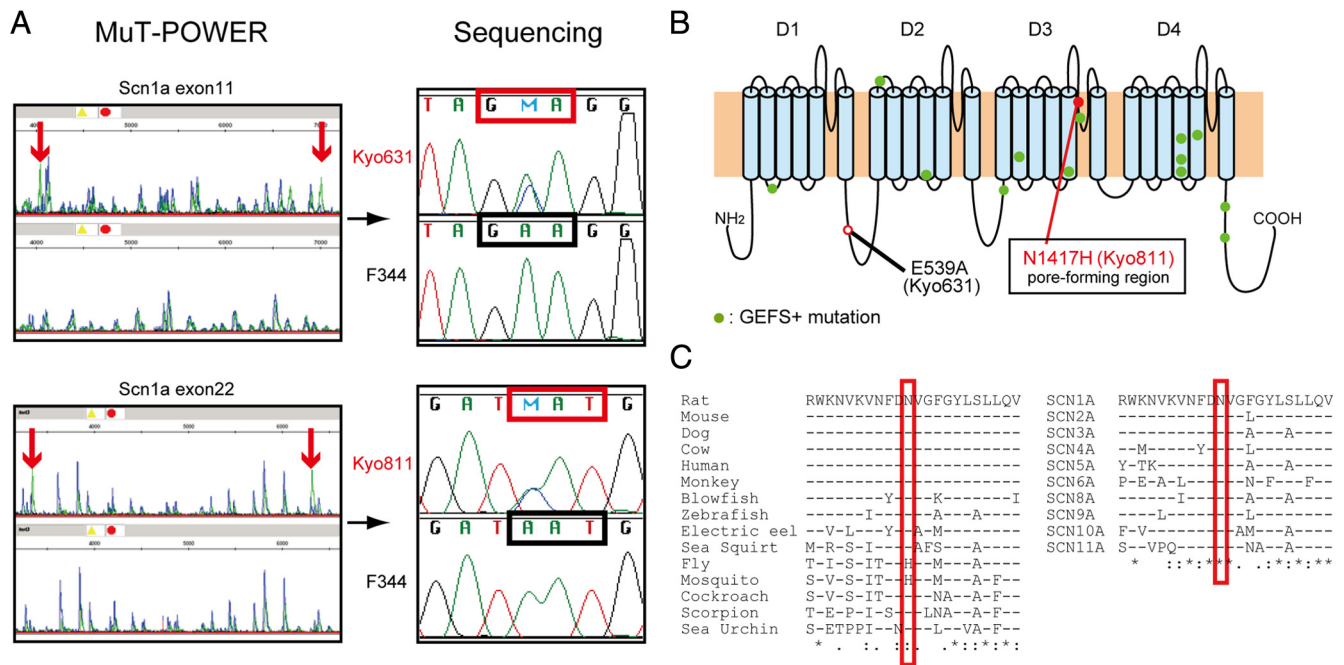


**Figure 1.** Identification of two mutations for the rat *Scn1a* gene (*Na<sub>v</sub>1.1*) by MuT-POWER screening of G<sub>1</sub> rats. **A**, Two positive peaks were detected with the primer sets amplifying exons 11 and 22 of the rat *Scn1a* gene. Both mutations were confirmed in individual Kyo631 and Kyo811 G<sub>1</sub> samples, respectively, by sequencing. Mutations appear as green peaks and are indicated with red arrows. Other overlapping green and blue peaks are background. **B**, N1417H was located in the third pore region of the sodium channel. **C**, N1417H is highly conserved among other species as well as in other genes encoding a sodium channel. Fly and mosquito have the same amino acid change of Kyo811, suggesting functional differences in channels from these species compared with vertebrates.

POWER for mutations at the rat locus orthologous to the human *SCN1A* gene, we were able to identify two mutations: Kyo631 and Kyo811 (Fig. 1A). Sequence analysis revealed that these two mutations were both single-nucleotide substitutions, A1616C and A4246C, resulting in amino acid changes, E539A and N1417H, respectively. The SIFT prediction (<http://blocks.fhcrc.org/sift/SIFT.html>) suggested that the N1417H substitution may markedly affect protein function. N1417H mutation is located in the pore region of the sodium channel in a domain that is highly conserved among other species as well as in other genes of the sodium channel family (Fig. 1C).

The recovery of two identified mutant rats, Kyo631 and Kyo811, from frozen sperm cells was achieved by ICSI, yielding 24 live rats, of which 6 and 5 rats, respectively, were confirmed heterozygous for the mutations by direct sequencing (supplemental Table 2, available at [www.jneurosci.org](http://www.jneurosci.org) as supplemental material). To eliminate mutations that might have been generated by ENU in other chromosomal regions of the *Scn1a* locus, more than five backcross generations were performed against the F344/NSlc inbred background. Heterozygous carriers were then intercrossed to produce homozygous individuals for both *Scn1a*<sup>Kyo631</sup> and *Scn1a*<sup>Kyo811</sup> alleles. Although the occurrence of a very tightly linked mutation with a phenotypic effect is very small, this possibility should be taken into account when designing the experiment and interpreting the results. We therefore compared littermates to validate the effect of the observed mutation. Both *Scn1a*<sup>Kyo631</sup> and *Scn1a*<sup>Kyo811</sup> strains appeared phenotypically normal without any obvious seizures. There were no apparent histological abnormalities in the brains of both rats. Since human GEFS+ patients exhibit various forms of clinically recognized seizures, including tonic-clonic, absence, and myoclonic seizures (Scheffer and Berkovic, 1997), we tested the sensitivity of *Scn1a* rats to seizures induced by the convulsant PTZ, a

GABA<sub>A</sub> receptor–chloride channel complex blocker. Rats homozygous F344-*Scn1a*<sup>Kyo811/Kyo811</sup> showed much higher susceptibility to PTZ than F344/NSlc, F344-*Scn1a*<sup>Kyo631/Kyo631</sup>, and heterozygous F344-*Scn1a*<sup>Kyo811/+</sup> (Fig. 2A; supplemental Table 3, available at [www.jneurosci.org](http://www.jneurosci.org) as supplemental material).

### Susceptibility to HIS

The most common symptoms of GEFS+ are FS and FS plus, in which the seizures are triggered by hyperthermia and occur after 6 years of age (Scheffer and Berkovic, 1997; Baulac et al., 1999). To investigate whether *Scn1a* mutant rats are susceptible to thermal stimuli, we used a hot water bath to induce FS (Klauenberg and Sparber, 1984). F344/NSlc and F344-*Scn1a*<sup>Kyo631/Kyo631</sup> rats at 5 weeks of age showed no seizures when exposed to 45°C hot water for 5 min, whereas all homozygous F344-*Scn1a*<sup>Kyo811/Kyo811</sup> rats (*n* = 11) exhibited clonic seizures with an average latency of 3.5 ± 0.6 min after immersion in water (Fig. 2B). Two of 11 *Scn1a*<sup>Kyo811/+</sup> heterozygous rats showed clonic seizures with a latency of 4.7 ± 0.4 min. Rectal temperature of the homozygous rats at seizure induction (43.3 ± 0.3°C) was significantly lower than that of heterozygous rats (44.2 ± 0.7°C; *p* < 0.007). We considered that the brain temperature could be lower than the rectal temperature that was measured when inducing the seizures, since the head of each rat was not submerged in the heated bath. Wild, heterozygous, and homozygous rats showed no difference for a normal rectal temperature of 37.9–38.3°C. Immersing these rats in 37–40°C water did not evoke seizures.

The convulsive seizures of homozygous rats persisted even after removal from the water bath with an average duration of 1.8 ± 0.7 min with several recurrences (Fig. 2B). These intermittent seizures typically consisted of tonic flexion, clonic convulsion, wet dog shake, myoclonic jerks of the limbs, straub tail, and oral automatisms (supplemental Video 1, avail-

able at [www.jneurosci.org](http://www.jneurosci.org) as supplemental material). Cortical EEG recording indicated complete correlation in the occurrence between behavioral seizures and paroxysmal epileptiform discharges (Fig. 2C). These HISs were abolished ( $n = 7$ ) by pretreatment of animals with diazepam (0.5 mg/kg, i.p.) (Fig. 2B), which is usually used as efficient treatment for FS in humans. These results indicate that the N1417H mutation within the pore region of *Scn1a* significantly increases susceptibility to experimental FS; therefore, we designated these hyperthermia-induced seizure-susceptible rats as “Hiss” rats.

### Age-dependent susceptibility to HIS

In rodent models of FS, postnatal day 8 (P8) to P14 rats are most susceptible to HIS (Chen et al., 1999; Schuchmann et al., 2006). To clarify the relationship between *Scn1a* expression and susceptibility to HIS, we monitored the expression level of *Scn1a* and hot water-induced seizures at 1–10 weeks of age (Fig. 3; supplemental Table 4, available at [www.jneurosci.org](http://www.jneurosci.org) as supplemental material). Throughout the entire course of the experiments, the expression levels of *Scn1a* in the brain were similar between Hiss (*Scn1a*<sup>Kyo811/Kyo811</sup>) and control F344/NSlc rats. At 1 and 2 weeks of age, *Scn1a* expression was very low (Fig. 3A, B), and the immersion of rats into 45°C water led to convulsive seizures in both F344/NSlc and Hiss rats (Fig. 3C). Seizures in such infantile rats, consisting of oral automatisms, myoclonic jerks of the limbs, and clonic convulsion, are generally milder than those seen in adult rats, and no sustained seizures were observed after removal from the water bath. No significant difference was observed between the two strains for apparent behavioral seizures and in the threshold temperature of seizure induction (supplemental Table 4, available at [www.jneurosci.org](http://www.jneurosci.org) as supplemental material).

At 3–5 weeks of age, *Scn1a* expression markedly increased and peaked at 5 weeks of age (Fig. 3A, B) in agreement with previous reports (Beckh et al., 1989; Gong et al., 1999). Susceptibility to HIS decreased with age and inversely with the increased expression of *Scn1a* in F344/NSlc rats (Fig. 3A, B), whereas the susceptibility remained in Hiss rats even at 10 weeks of age (Fig. 3C). In Hiss rats, sustained seizures were observed at 3, 5, and 10 weeks of age. Rectal temperature at seizure induction in Hiss rats was significantly lower than in control F344/NSlc rats (supplemental Table 4, available at [www.jneurosci.org](http://www.jneurosci.org) as supplemental material).

### Electrophysiological properties of the N1417H channel

To investigate how the N1417H missense mutation affects neuronal activities, we examined the electrophysiological properties of the N1417H mutation using a heterologous expression system in human HEK293 cells (Lossin et al., 2002; Ohmori et al., 2006). Cells expressing the N1417H mutant channels exhibited a voltage-dependent inward current that resembled cells transfected with WT channels (Fig. 4A). Inactivation proceeded in a rapid biexponential manner, with no apparent difference be-

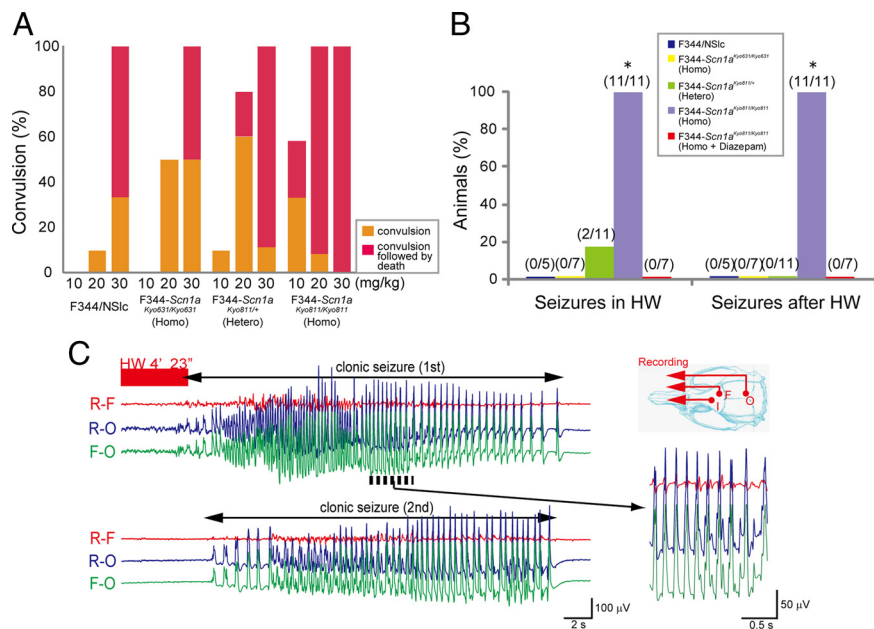


**Figure 2.** Susceptibility of *Scn1a* rats to PTZ and hyperthermia stimuli. **A**, All strains exhibited dose-dependent PTZ-induced seizures, but susceptibility was increased slightly in heterozygous *Scn1a*<sup>Kyo811/+</sup> rats and significantly in homozygous *Scn1a*<sup>Kyo811/Kyo811</sup>. The numbers of rats are described in supplemental Table 3 (available at [www.jneurosci.org](http://www.jneurosci.org) as supplemental material). **B**, Quantitative analysis of the number of rats developing clonic seizures induced by hyperthermia in hot water (left) and extended convulsive seizures after taking them out of the water (right). The numbers of rats are indicated in parentheses. \* $p < 0.01$ . **C**, Typical epileptic discharges during convulsion induced by hyperthermia (red bar) in the temporal cortex of homozygous rats at 5 weeks of age during clonic convulsion. The clonic convulsive seizures of homozygous rats extended after taking them out of the water with a few recurrences. In some homozygous rats, transient tonic convulsions were observed during clonic seizures. The insets show generalized cortical seizures on an expanded scale. F, Frontal cortex; O, occipital cortex; I, indifferent electrode.

tween WT and N1417H (Fig. 4B). N1417H channels showed no difference in current density and voltage dependence channel activation compared with WT (Fig. 4C, D); however, N1417H exhibited a significant hyperpolarizing shift in half-maximal steady-state inactivation (Fig. 4E; supplemental Table 5, available at [www.jneurosci.org](http://www.jneurosci.org) as supplemental material). Moreover, recovery from fast inactivation was significantly slower in N1417H-expressing cells ( $p < 0.05$ ) (Fig. 4F).

In previous reports, increased persistent sodium currents were observed in epilepsy-associated *Scn1a* mutant channels (Lossin et al., 2002; Meisler and Kearney, 2005; Stafstrom, 2007). Figure 4G illustrates representative, tetrodotoxin-subtracted current traces for WT-SCN1A and N1417H in response to a 100 mV voltage step to  $-10$  mV from a holding potential of  $-120$  mV. Cells expressing N1417H exhibited a significantly greater persistent current expressed as a percentage of peak current ( $0.88 \pm 0.17\%$ ;  $n = 11$ ) compared with WT-SCN1A ( $0.38 \pm 0.10\%$ ;  $n = 7$ ;  $p < 0.05$ ) (Fig. 4H).

### Sodium channel properties in hippocampal neurons

To access functional properties in native N1417H channels, we examined whole-cell sodium currents in hippocampal pyramidal cells (glutamatergic neurons) and bipolar cells (GABAergic interneurons) dissociated from 12- to 16-d-old F344/NSlc and Hiss rats (*Scn1a*<sup>Kyo811/Scn1a</sup><sup>Kyo811</sup>). Whole-cell sodium currents recorded in pyramidal cells from F344/NSlc and Hiss rats were similar in current density, voltage dependence of activation, and voltage dependence of inactivation (supplemental Fig. 1, Table 6, available at [www.jneurosci.org](http://www.jneurosci.org) as supplemental material). In bipolar cells, the mean current amplitudes, capacitance, and densities were not significantly different between F344/NSlc and Hiss

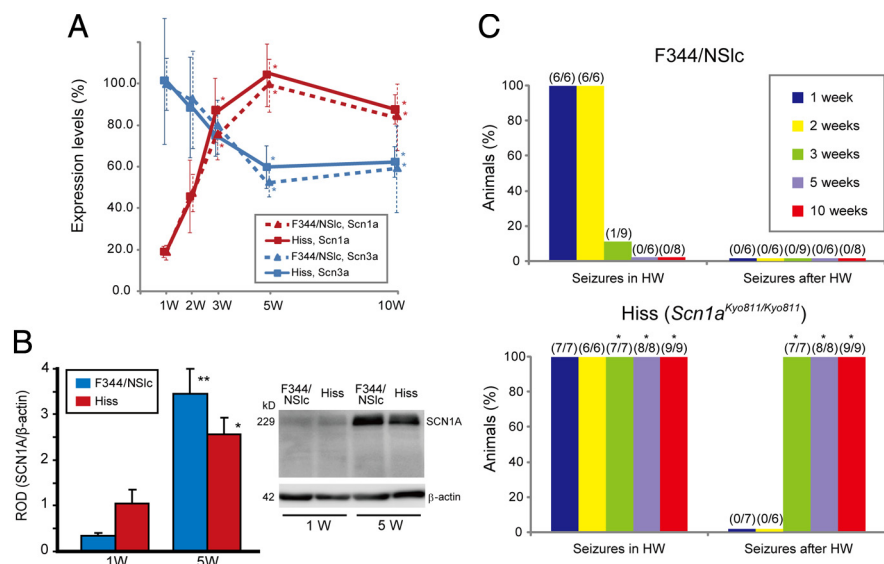


**Figure 3.** Developmental changes in *Scn1a* expression and susceptibility to hyperthermia-induced seizures. **A**, *Scn1a* (red) and *Scn3a* (blue) mRNA quantification was expressed as a percentage of the maximum level, at different postnatal ages, 1–10 weeks, in the brain of F344/NSlc (triangle) and Hiss (rectangle) rats. Error bars indicate mean  $\pm$  SE. \* $p < 0.05$  for each age versus 1 week by ANOVA. **B**, Na<sub>v</sub>1.1 protein levels in the hippocampus of F344/NSlc (blue) and Hiss (red) rats at 1 and 5 weeks of age. The expression level was normalized against  $\beta$ -actin. \* $p < 0.05$  and \*\* $p < 0.01$  for 1 week versus 5 weeks by Student's *t* test. **C**, Quantitative analysis of the number of rats developing clonic seizures induced by hyperthermia in hot water (left) and extended convulsive seizures after taking them out of the water (right), at different postnatal ages 1–10 weeks, for F344/NSlc (top) and Hiss (bottom) rats. The numbers of rats are indicated in parentheses. \* $p < 0.01$  versus F344/NSlc.

rats (Fig. 5A–C). Voltage dependence of activation was not different between F344/NSlc and Hiss rats, whereas inactivation showed different voltage dependence, in which the curve significantly shifted in the hyperpolarizing direction in Hiss rats (Fig. 5D,E; supplemental Table 7, available at www.jneurosci.org as supplemental material). The mean inactivation time constants were not different between F344/NSlc and Hiss rats (Fig. 5F). Persistent sodium currents, evaluated during the final 10 ms of a 100 ms depolarization to  $-30$  mV, were significantly increased in hippocampal bipolar cells of Hiss rats ( $p < 0.05$ ) (Fig. 5G,H).

We examined how these abnormal properties of the sodium channels affected neuronal firing patterns. We recorded the action potentials that originated from dissociated hippocampal pyramidal neurons and bipolar neurons in response to a series of current injections and determined the input–output relationship. The number of action potentials and their firing patterns were similar for pyramidal neurons from F344/NSlc and Hiss rats (supplemental Fig. 2, available at www.jneurosci.org as supplemental material). The number of action potentials for bipolar cells was similar, but was slightly reduced for Hiss rats with increasing injected current (Fig. 6A,B). At 95 pA injected current, the first and last spike amplitudes of the action potential were significantly reduced for Hiss rats (Fig. 6C). The width of their firing patterns was slightly broader at 95 pA injected current (Fig. 6D). These results indicate that interneuron excitability was slightly reduced in the hippocampus of the Hiss rat.

## Discussion

Animal models of FS have been previously established. For these, convulsive activity is evoked by exposing rats to hyperthermia, which increases their body temperature to a level that is comparable with a human fever. Methods include using heated air (Holtzman et al., 1981; Chen et al., 1999; Schuchmann et al., 2006), jets of hot water that are applied to the head (Ullal et al.,

1996), or through bathing in hot water (Klaunberg and Sparber, 1984). These models permitted fundamental discoveries about their underlying mechanisms and consequences for developing epilepsy. However, significant gaps in our knowledge remain regarding the role of genetic predispositions toward FS, which has often been observed in human families. In this study, by using the ENU mutagenesis approach, we generated *Scn1a*-targeted Hiss rats. The rats carried a N1417H missense mutation in the third pore region of the sodium channel, in which several mutations have been reported for SMEI and GEFS+ families (Sugawara et al., 2001; Lossin, 2009). Using this model, we found that the Na<sub>v</sub>1.1 channel plays an important role in controlling experimental FS. To our knowledge, the Hiss rat is the first animal model of FS that combines experimental FS models, such as hyperthermia-induced seizures, with a genetic predisposition, a missense mutation in the Na<sub>v</sub>1.1 gene.

FS in humans is clearly age dependent in children between 6 months and 6 years of age, whereas P8–P14 rats are most susceptible to experimental FS (Holtzman et al., 1981; Chen et al., 1999; Schuchmann et al., 2006). Although superimposing the developmental stages of the rodent brain onto those of the human brain is difficult, the P12–P13 rat seems to correspond to a full-term human neonate (Romijn et al., 1991). The transiently high susceptibility to experimental FS that is seen for rats can be expected to occur before birth for humans, when GABAergic inhibition is relatively immature. During the first two postnatal weeks for rats and most likely during the late prenatal and early postnatal period for humans, GABA promotes a paradoxical excitatory activity. This is attributable to a larger intracellular Cl<sup>−</sup> concentration, which depolarizes neurons (Ben-Ari and Holmes, 2006). The shift from a depolarizing to hyperpolarizing Cl<sup>−</sup> concentration simultaneously occurs at P14 for rats with a decrease in NKCC1 cotransporter expression. This facilitates Cl<sup>−</sup> accumulation in neurons and increased KCC2 cotransporter expression, which extrudes intracellular Cl<sup>−</sup> (Dzhala et al., 2005). The age-dependent expression patterns of NKCC1 and KCC2 are quite similar to those of *Scn3a* and *Scn1a*, respectively, which we observed in this study (Fig. 3). Moreover, the susceptibility of F344 rats to HIS disappeared after 3 weeks of age in parallel with *Scn1a* expression. However, the Hiss rats remained susceptible probably because of the impaired function of the mutated Na<sub>v</sub>1.1 channel. Generally, human FS occurs suddenly and without any obvious symptoms, except for a rapid rise of fever usually within 24 h of fever onset. The Hiss rat displays a typical convulsive seizure when its body temperature reaches a certain threshold, with extended seizures occurring after being removed from hot water (supplemental Video 1, available at www.jneurosci.org as supplemental material). Human and rat FSs are effectively prevented by using anticonvulsants such as diazepam. Considering the behavioral similarity of the seizures and the neuronal developmental conditions in the brain, the Hiss rat is a useful animal model of human FS and FS+. It will therefore enable a better understanding of the etiology of FS and/or associated epilepsy.

GEFS+ is a familial epilepsy syndrome for which the majority of patients present with typical FS or FS+. In addition, patients can have afebrile seizures, including generalized tonic–clonic seizures, myoclonic seizures, atonic seizures, or myoclonic–astatic epilepsy (Scheffer and Berkovic, 1997). For Hiss rats, obvious spontaneous seizures are very rare. Only a few cases of typical tonic–clonic seizures have been observed for adults. The potential contribution of FS to temporal lobe epilepsy is a topic of interest (Baulac et al., 2004; Dubé et al., 2007; Sadleir and Scheffer, 2007). Prospective studies suggested that a history of long or complex FSs significantly increases the risk for epilepsy. However, the precise mechanisms that mediate early-life epileptogenesis remain unknown. Animal models of FS show that experimentally prolonged FS elicits long-lasting changes in neuronal function, which might lead to limbic epilepsy (Dubé et al., 2006). For Hiss rats, neither prolonged experimental FS nor repetitive FS between 3 and 5 weeks of age evoked obvious epileptic seizures in the adults. However, this should be investigated in better detail using more sophisticated equipment. For example, a systematic video-EEG monitoring system could be used to detect spontaneous seizures, which might rarely occur in the adults.

Hyperthermia does not encompass the spectrum of biological processes of FS. However, temperature influences numerous cellular processes, including the activities of several types of neuronal ion channels and the electrical activity of neurons. This could enhance the rate, magnitude, or synchrony of neuronal firing and lead to seizures (Hodgkin and Katz, 1949; Moser et al., 1993). This is supported by the observation that FS was induced for Japanese patients who bathed in hot water (Fukuda et al., 1997). Some authors have also reported a considerable coexistence of FS of 5–15% for family histories of patients who suffer from hot water epilepsy (Mani et al., 1974; Satishchandra, 2003). Evidence exists that hyperthermia per se triggers seizures *in vivo* (Chen et al., 1999; Schuchmann et al., 2006) and induces epileptiform activity *in vitro* (Wu et al., 2001). For one *in vivo* model, increased body temperature for rat pups leads to a pronounced increase in the respiration rate. This is followed by an increase in brain pH, which triggers ictal activity, also known as respiratory alkalosis (Schuchmann et al., 2006). It would be interesting to study whether the  $\text{Na}_v1.1$  channel mutation influences the pH sensitivity of the brain,

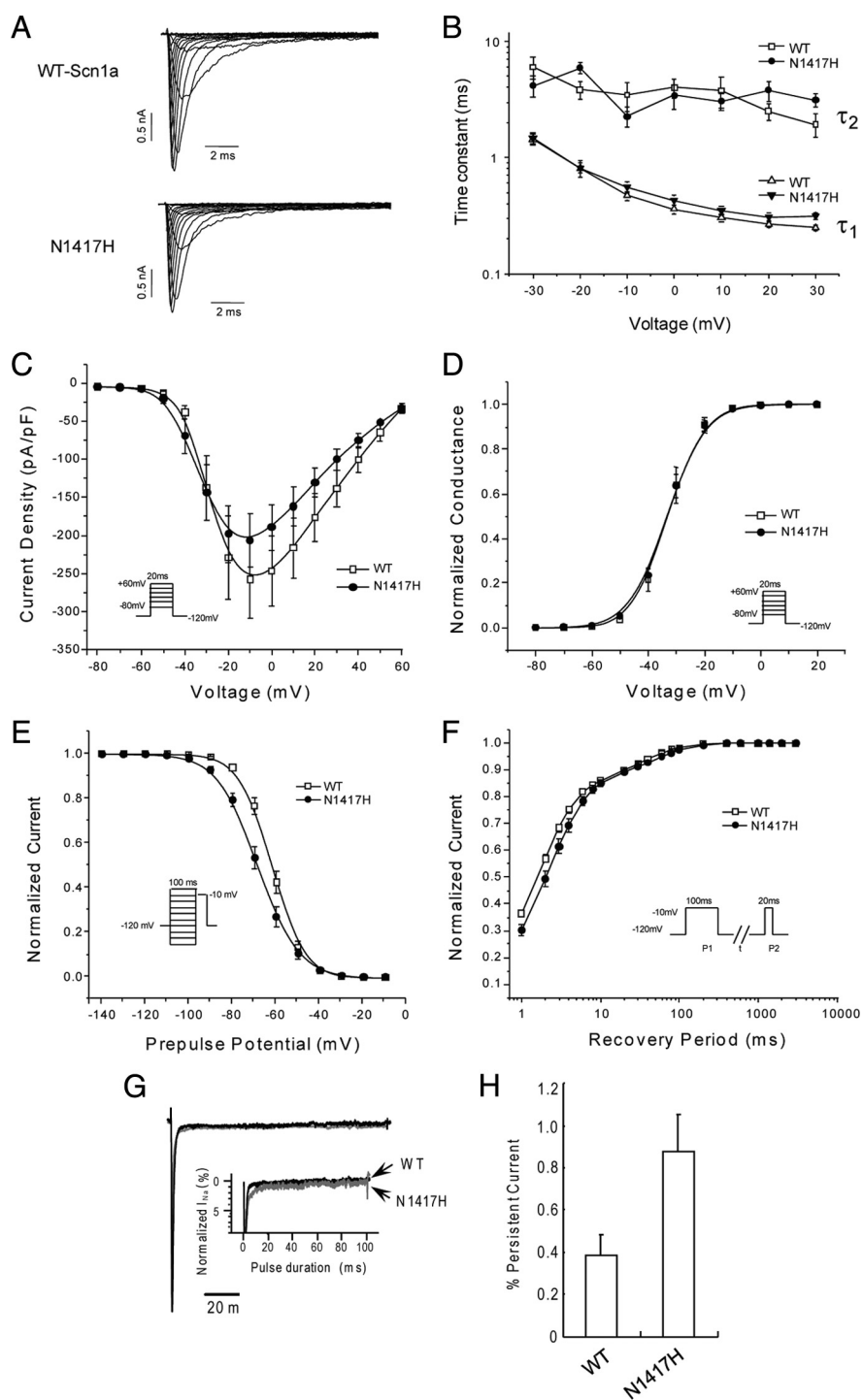


**Figure 4.** Sodium currents recorded from HEK293 cells expressing either WT-SCN1A or N1417H. **A**, Representative whole-cell sodium currents. The currents were activated by voltage steps to between  $-80$  and  $+60$  mV in  $20$  mV increments from a holding potential of  $-120$  mV. **B**, Voltage dependence of fast inactivation time constants for WT-SCN1A and N1417H. Fast and slow time constants were plotted versus voltage. **C**, Peak current density of whole-cell currents elicited by test pulses to various potentials and normalized to cell capacitance. WT,  $n = 8$ ; N1417H,  $n = 10$ . **D**, Voltage dependence of channel activation measured during voltage steps to between  $-80$  and  $+20$  mV from a holding potential of  $-120$  mV. **E**, Voltage dependence of fast inactivation measured at  $-10$  mV in response to a  $100$  ms prepulse voltage step to between  $-140$  and  $-10$  mV from a holding potential of  $-120$  mV. **F**, Recovery from fast inactivation was evaluated using a two-pulse protocol, and the data were fitted with a two-exponential function. Time-dependent recovery from fast inactivation measured at  $-10$  mV between  $1$  and  $3000$  ms immediately after a  $100$  ms prepulse voltage step to  $-10$  mV from a holding potential of  $-120$  mV. **G**, Representative tetrodotoxin-subtracted whole-cell sodium currents recorded from HEK293 cells expressing WT-SCN1A and N1417H. Persistent current was measured in response to a  $100$  ms voltage step to  $-10$  mV from a holding potential of  $-120$  mV. Each current trace has been normalized to its peak sodium current. The inset shows an expanded  $y$ -axis scaled to emphasize the relative proportion of persistent current. **H**, Quantification of persistent current as a percentage of peak current for WT ( $n = 7$ ) and N1417H ( $n = 7$ ). Error bars indicate mean  $\pm$  SE.

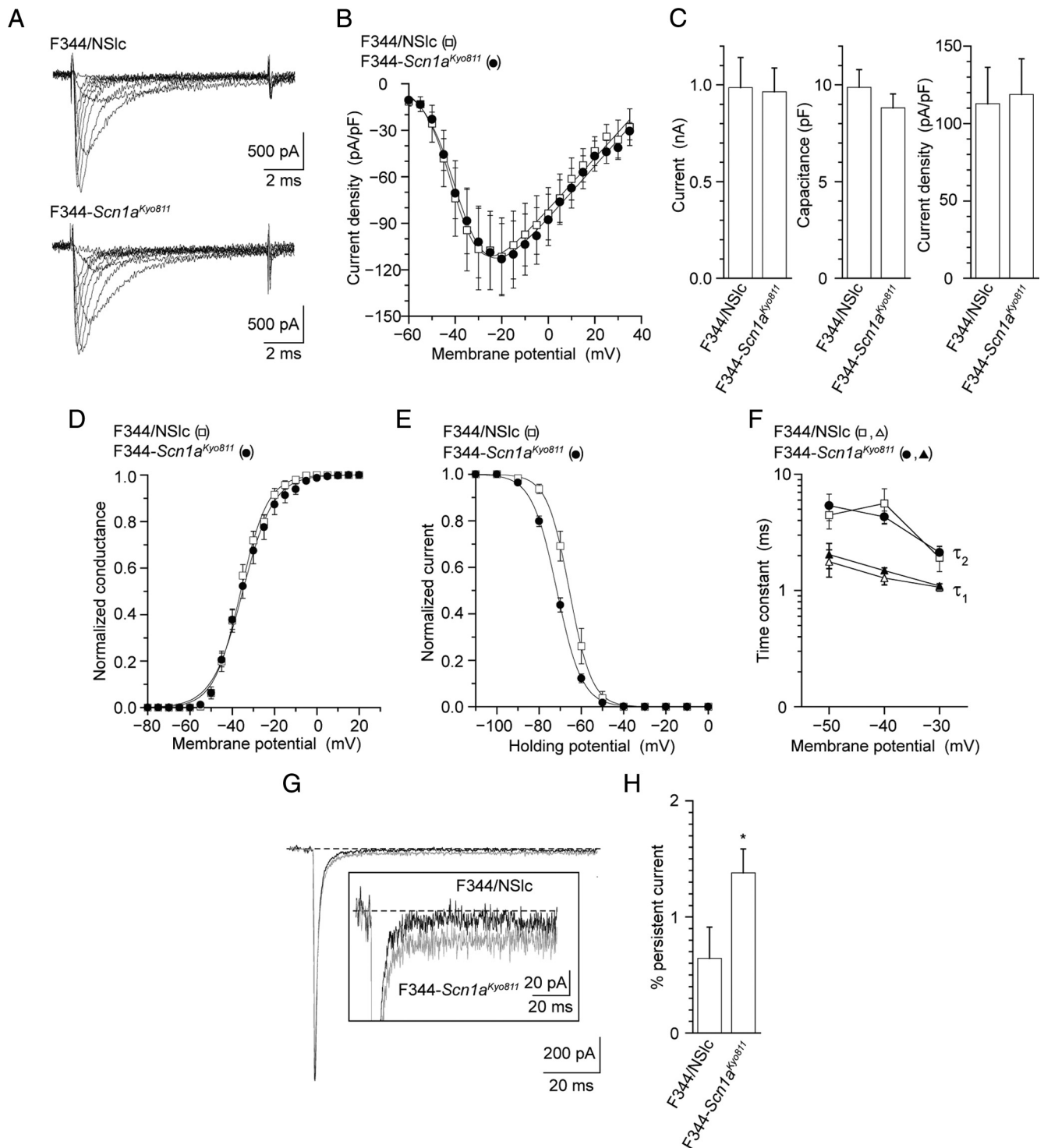


**Figure 5.** Comparison of sodium currents recorded in hippocampal bipolar neurons dissociated from F344/NSlc and Hiss rats. **A**, Families of sodium currents evoked by  $10$  ms depolarizing pulses from  $-60$  to  $20$  mV with  $10$  mV increments at a  $V_h$  of  $-100$  mV in hippocampal bipolar neurons dissociated from F344/NSlc (top) and Hiss (bottom) rats. **B**,  $I$ - $V$  relationships for F344/NSlc (open squares;  $n = 8$ ) and Hiss (filled circles;  $n = 14$ ). **C**, Comparison of peak current amplitudes (left), cell capacitances (middle), and current densities (right). Sodium currents elicited by a step pulse from a  $V_h$  of  $-100$  to  $-20$  mV are analyzed. Means  $\pm$  SE are shown. **D**, Voltage dependence of activation for F344/NSlc (open squares;  $n = 8$ ) and Hiss (filled circles;  $n = 14$ ). Half-maximal activation occurred at  $-37.4 \pm 1.3$  mV with a slope factor of  $6.6 \pm 0.3$  for F344/NSlc and at  $-36.5 \pm 1.8$  mV with a slope factor of  $6.6 \pm 0.2$  for Hiss. **E**, Voltage dependence of inactivation for F344/NSlc (open squares;  $n = 5$ ) and Hiss (filled circles;  $n = 13$ ). Amplitudes of currents evoked by the test pulse to  $-20$  mV after a  $100$  ms  $V_h$  prepulse to various membrane potentials between  $-110$  and  $0$  mV were normalized to the current amplitude induced by the test pulse after a  $100$  ms  $V_h$  prepulse of  $-100$  mV. The mean values were plotted as a function of potentials of  $100$  ms  $V_h$  prepulse and were fitted to the Boltzmann equation. Membrane potentials for half-maximal inactivation and slope factors were as follows: F344/NSlc,  $-65.6 \pm 1.8$  mV and  $-4.8 \pm 0.3$ ; Hiss,  $-71.5 \pm 0.8$  mV ( $p < 0.05$ ) and  $-5.7 \pm 0.2$  ( $p < 0.05$ ). **F**, Inactivation time constants of hippocampal bipolar neurons from F344/NSlc (open symbols;  $n = 21$ ) and Hiss (filled symbols;  $n = 23$ ). Current decay was fitted by a sum of two exponential functions. The mean inactivation time constants for fast  $\tau_1$  (open triangles and filled triangles) and slow  $\tau_2$  (open squares and filled circles) were plotted as a function of test potentials from  $-50$  to  $-30$  mV. **G**, Representative sodium current was evoked by  $100$  ms depolarization to  $-30$  mV from  $V_h$ . TTX-sensitive currents were obtained by digital subtraction of sodium currents recorded before and after  $1 \mu\text{M}$  TTX addition. The inset shows an expanded vertical scale to emphasize the relative proportion of the persistent current. **H**, Persistent sodium currents in hippocampal bipolar neurons from F344/NSlc ( $n = 17$ ) and Hiss ( $n = 12$ ). Persistent current was evaluated during the final  $10$  ms of  $100$  ms depolarization to  $-30$  mV. Error bars indicate mean  $\pm$  SE if larger than symbols. \* $p < 0.05$  versus F344/NSlc.



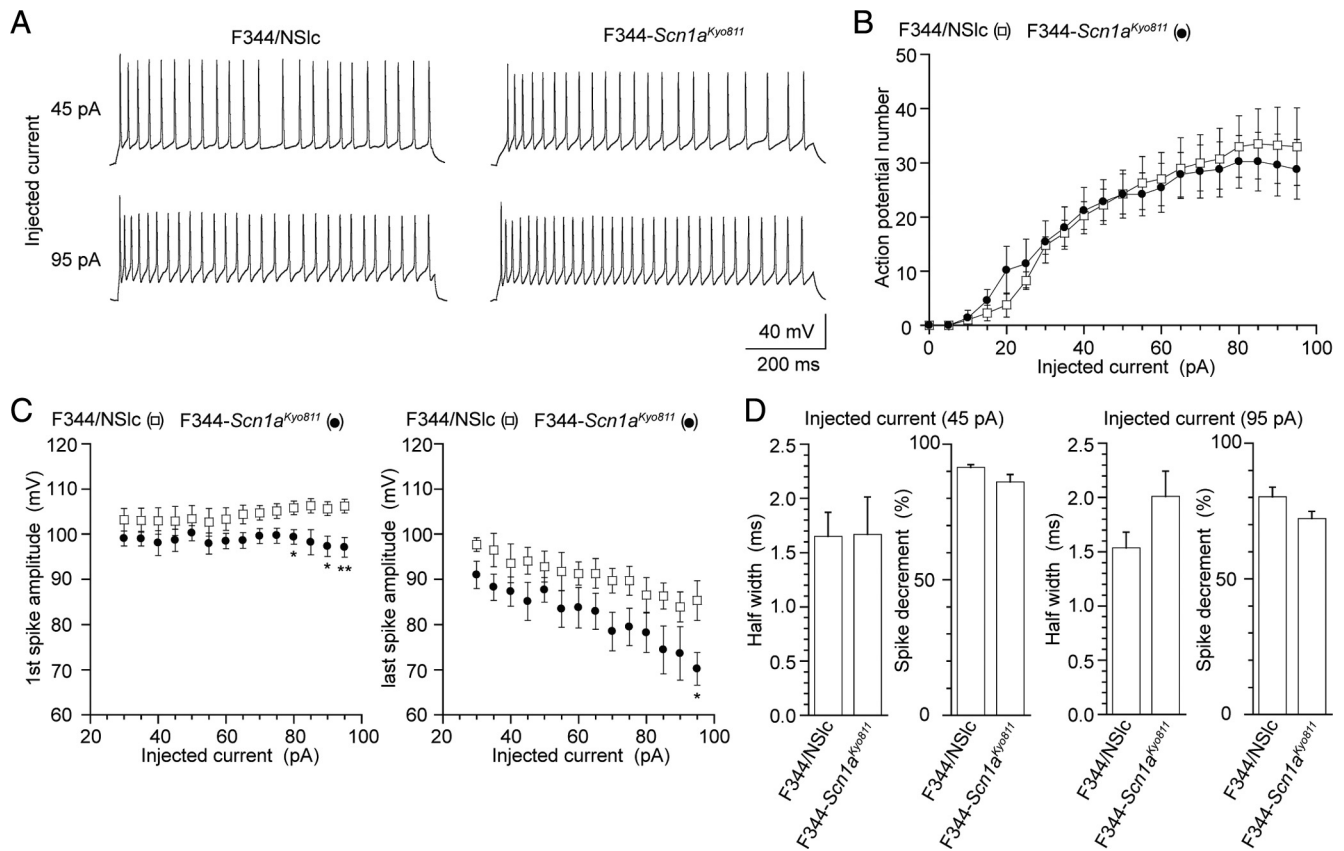


**Figure 6.** Depolarization-evoked firing activity of hippocampal bipolar neurons that have been dissociated from F344/NSlc and Hiss rats. **A**, Representative sets of action potential traces recorded for F344/NSlc and Hiss hippocampal bipolar neurons during 800 ms injections of 45 pA (top) and 95 pA of current (bottom), for a membrane potential of  $-80$  mV. **B**, Input–output relationship for the number of action potentials elicited versus the injected current for F344/NSlc (open squares;  $n = 4$ ) and Hiss (filled circles;  $n = 5$ ). **C**, Spike amplitudes of the first (left) and last (right) action potentials elicited versus the injected current for F344/NSlc ( $n = 4$ ) and Hiss ( $n = 5$ ) hippocampal bipolar neurons. **D**, Half-width of the first action potentials and spike decrement for F344/NSlc ( $n = 4$ ) and Hiss ( $n = 5$ ) hippocampal bipolar neurons elicited by 45 pA (left) and 95 pA of current injection (right). The spike decrement was calculated as the percentage of the last spike amplitude divided by the first spike amplitude. Means  $\pm$  SE are shown. \* $p < 0.01$ , \*\* $p < 0.01$  versus F344/NSlc.

which may involve neuronal mechanisms that control respiration and acid–base homeostasis.

Several missense mutations in the  $\text{Na}_v1.1$  channel have been reported for GEFS+. A couple of studies used recombinant  $\text{Na}_v1.1$  channels and electrophysiological recordings. They revealed that these mutations may cause either gain-of-function or loss-of-function effects that are consistent with either increased or decreased neuronal excitability (Ragsdale, 2008; Lossin, 2009). Our observations that were based on the electrophysiological analysis of the  $\text{Na}_v1.1$  channel in heterologously expressed HEK cells indicated that the N1417H missense mutation has a hyperpolarized shift for the voltage dependence of fast inactivation. These results were confirmed for isolated hippocampal interneurons, but not for pyramidal neurons, from Hiss rats. The N1417H missense mutation may decrease the availability of the  $\text{Na}_v1.1$  channel in inhibitory interneurons, resulting in the partial dysfunction of network inhibition. Interestingly, the M145T mutation of SCN1A linked to simple FS was reported on for a large family (Baulac et al., 2004; Mantegazza et al., 2005; Colosimo et al., 2007). This is consistent with other reports that found a link with the FEB3 locus of FS families (Peiffer et al., 1999; Baulac and Baulac, 2009). The phenotypes and genetic conditions of the Hiss rat seem to be very similar to those reported for simple FS patients of the M145T family. Of note, the M145T mutation causes a partial loss of function.

A persistent current causes neuronal hyperexcitability, for which the channels do not stably inactivate and the sodium cur-

rents of mutant cells fail to completely decay to the baseline (Lossin et al., 2002; Meisler and Kearney, 2005; Stafstrom, 2007). Although this abnormal and persistent current represents only a fraction of the peak transient current, it persists long after the transient current has been inactivated. This may profoundly affect neuronal excitability. For our heterologous expression system of HEK cells, the N1417H missense mutation resulted in a slightly but significantly increased persistent current compared with the wild-type channel. This persistent sodium current was confirmed for hippocampal bipolar neurons, but not for pyramidal neurons in Hiss rats. The  $\text{Na}_v1.1$  channel is predominantly expressed in hippocampal interneurons (Yu et al., 2006; Ogiwara et al., 2007) and also is expressed at lower levels in pyramidal neurons (Tang et al., 2009). We could not clarify whether the persistent sodium current can increase or decrease the excitability of hippocampal neurons. In fact, the combination of opposing biophysical properties, namely the predicted gain and loss of channel activity, has been reported for GEFS+ and related epileptic syndrome-associated SCN1A mutations (Lossin et al., 2002; Rhodes et al., 2005; Ohmori et al., 2006). Our current-clamp recordings clearly showed a reduction in the action potential amplitude for the hippocampal interneurons of Hiss rats. A larger reduction was observed with increasing injected current. This may be associated with enhanced susceptibility to febrile seizures for Hiss rats because of the reduced inhibition of GABAergic interneurons. The resulting dysfunction of network

inhibition can hyperactivate excitatory pyramidal neurons during acute hyperthermia. We could not, however, rule out that other sodium channels, such as  $\text{Na}_v1.3$  channels, may affect the firing activities of the hippocampus of the mutant rats.

In conclusion, our studies, which used a rat model of FS, revealed that the impaired biophysical properties of hippocampal interneurons contribute to susceptibility to FS among rats. Hiss rats can be used to test the effects of preventative new drugs against FS, FS+, and/or associated epilepsy.

## References

- Baulac S, Baulac M (2009) Advances on the genetics of mendelian idiopathic epilepsies. *Neurol Clin* 27:1041–1061.
- Baulac S, Gourfinkel-An I, Picard F, Rosenberg-Bourgin M, Prud'homme JF, Baulac M, Brice A, LeGuern E (1999) A second locus for familial generalized epilepsy with febrile seizures plus maps to chromosome 2q21-q33. *Am J Hum Genet* 65:1078–1085.
- Baulac S, Gourfinkel-An I, Nabbout R, Huberfeld G, Serratosa J, Leguern E, Baulac M (2004) Fever, genes, and epilepsy. *Lancet Neurol* 3:421–430.
- Beckh S, Noda M, Lübbert H, Numa S (1989) Differential regulation of three sodium channel messenger RNAs in the rat central nervous system during development. *EMBO J* 8:3611–3616.
- Ben-Ari Y, Holmes GL (2006) Effects of seizures on developmental processes in the immature brain. *Lancet Neurol* 5:1055–1063.
- Chen K, Baram TZ, Soltesz I (1999) Febrile seizures in the developing brain result in persistent modification of neuronal excitability in limbic circuits. *Nat Med* 5:888–894.
- Colosimo E, Gambardella A, Mantegazza M, Labate A, Rusconi R, Schiavon E, Annesi F, Cassulini RR, Carrideo S, Chifari R, Canevini MP, Canger R, Franceschetti S, Annesi G, Wanke E, Quattrone A (2007) Electroclinical features of a family with simple febrile seizures and temporal lobe epilepsy associated with SCN1A loss-of-function mutation. *Epilepsia* 48:1691–1696.
- Dravet C, Bureau M, Oguni H, Fukuyama Y, Cokar O (2005) Severe myoclonic epilepsy in infancy: Dravet syndrome. *Adv Neurol* 95:71–102.
- Dubé C, Richichi C, Bender RA, Chung G, Litt B, Baram TZ (2006) Temporal lobe epilepsy after experimental prolonged febrile seizures: prospective analysis. *Brain* 129:911–922.
- Dubé CM, Brewster AL, Richichi C, Zha Q, Baram TZ (2007) Fever, febrile seizures and epilepsy. *Trends Neurosci* 30:490–496.
- Dzhala VI, Talos DM, Sdrulla DA, Brumbaugh AC, Mathews GC, Benke TA, Delpire E, Jensen FE, Staley KJ (2005) NKCC1 transporter facilitates seizures in the developing brain. *Nat Med* 11:1205–1213.
- Fukuda M, Morimoto T, Nagao H, Kida K (1997) Clinical study of epilepsy with severe febrile seizures and seizures induced by hot water bath. *Brain Dev* 19:212–216.
- Gong B, Rhodes KJ, Bekele-Arcuri Z, Trimmer JS (1999) Type I and type II  $\text{Na}^+$  channel alpha-subunit polypeptides exhibit distinct spatial and temporal patterning, and association with auxiliary subunits in rat brain. *J Comp Neurol* 412:342–352.
- Hirabayashi M, Kato M, Aoto T, Sekimoto A, Ueda M, Miyoshi I, Kasai N, Hochi S (2002) Offspring derived from intracytoplasmic injection of transgenic rat sperm. *Transgenic Res* 11:221–228.
- Hodgkin AL, Katz B (1949) The effect of temperature on the electrical activity of the giant axon of the squid. *J Physiol* 109:240–249.
- Holtzman D, Obana K, Olson J (1981) Hyperthermia-induced seizures in the rat pup: a model for febrile convulsions in children. *Science* 213:1034–1036.
- Klaunberg BJ, Sparber SB (1984) A kindling-like effect induced by repeated exposure to heated water in rats. *Epilepsia* 25:292–301.
- Lossin C (2009) A catalog of SCN1A variants. *Brain Dev* 31:114–130.
- Lossin C, Wang DW, Rhodes TH, Vanoye CG, George AL Jr (2002) Molecular basis of an inherited epilepsy. *Neuron* 34:877–884.
- Mani KS, Mani AJ, Ramesh CK (1974) Hot-water epilepsy—a peculiar type of reflex epilepsy: clinical and EEG features in 108 cases. *Trans Am Neurol Assoc* 99:224–226.
- Mantegazza M, Gambardella A, Rusconi R, Schiavon E, Annesi F, Cassulini RR, Labate A, Carrideo S, Chifari R, Canevini MP, Canger R, Franceschetti S, Annesi G, Wanke E, Quattrone A (2005) Identification of an Nav1.1 sodium channel (SCN1A) loss-of-function mutation associated with familial simple febrile seizures. *Proc Natl Acad Sci U S A* 102:18177–18182.
- Mashimo T, Yanagihara K, Tokuda S, Voigt B, Takizawa A, Nakajima R, Kato M, Hirabayashi M, Kuramoto T, Serikawa T (2008) An ENU-induced mutant archive for gene targeting in rats. *Nat Genet* 40:514–515.
- Meisler MH, Kearney JA (2005) Sodium channel mutations in epilepsy and other neurological disorders. *J Clin Invest* 115:2010–2017.
- Moser E, Mathiesen I, Andersen P (1993) Association between brain temperature and dentate field potentials in exploring and swimming rats. *Science* 259:1324–1326.
- Mulley JC, Scheffer IE, Petrou S, Dibbens LM, Berkovic SF, Harkin LA (2005) SCN1A mutations and epilepsy. *Hum Mutat* 25:535–542.
- Nakayama J (2009) Progress in searching for the febrile seizure susceptibility genes. *Brain Dev* 31:359–365.
- Oakley JC, Kalume F, Yu FH, Scheuer T, Catterall WA (2009) Temperature- and age-dependent seizures in a mouse model of severe myoclonic epilepsy in infancy. *Proc Natl Acad Sci U S A* 106:3994–3999.
- Ogiwara I, Miyamoto H, Morita N, Atapour N, Mazaki E, Inoue I, Takeuchi T, Itohara S, Yanagawa Y, Obata K, Furuichi T, Hensch TK, Yamakawa K (2007)  $\text{Na}_v1.1$  localizes to axons of parvalbumin-positive inhibitory interneurons: a circuit basis for epileptic seizures in mice carrying an *Scn1a* gene mutation. *J Neurosci* 27:5903–5914.
- Ohmori I, Kahlig KM, Rhodes TH, Wang DW, George AL Jr (2006) Non-functional SCN1A is common in severe myoclonic epilepsy of infancy. *Epilepsia* 47:1636–1642.
- Peiffer A, Thompson J, Charlier C, Otterud B, Varvil T, Pappas C, Barnitz C, Gruenthal K, Kuhn R, Leppert M (1999) A locus for febrile seizures (FEB3) maps to chromosome 2q23–24. *Ann Neurol* 46:671–678.
- Ragsdale DS (2008) How do mutant Nav1.1 sodium channels cause epilepsy? *Brain Res Rev* 58:149–159.
- Rhodes TH, Vanoye CG, Ohmori I, Ogiwara I, Yamakawa K, George AL Jr (2005) Sodium channel dysfunction in intractable childhood epilepsy with generalized tonic-clonic seizures. *J Physiol* 569:433–445.
- Romijn HJ, Hofman MA, Gramsbergen A (1991) At what age is the developing cerebral cortex of the rat comparable to that of the full-term newborn human baby? *Early Hum Dev* 26:61–67.
- Sadleir LG, Scheffer IE (2007) Febrile seizures. *BMJ* 334:307–311.
- Satishchandra P (2003) Hot-water epilepsy. *Epilepsia* 44 [Suppl 1]:S29–S32.
- Scheffer IE, Berkovic SF (1997) Generalized epilepsy with febrile seizures plus. A genetic disorder with heterogeneous clinical phenotypes. *Brain* 120:479–490.
- Schuchmann S, Schmitz D, Rivera C, Vanhatalo S, Salmen B, Mackie K, Sipilä ST, Voipio J, Kaila K (2006) Experimental febrile seizures are precipitated by a hyperthermia-induced respiratory alkalosis. *Nat Med* 12:817–823.
- Stafstrom CE (2007) Persistent sodium current and its role in epilepsy. *Epilepsy Curr* 7:15–22.
- Sugawara T, Mazaki-Miyazaki E, Ito M, Nagafuji H, Fukuma G, Mitsudome A, Wada K, Kaneko S, Hirose S, Yamakawa K (2001) Nav1.1 mutations cause febrile seizures associated with afebrile partial seizures. *Neurology* 57:703–705.
- Tang B, Dutt K, Papale L, Rusconi R, Shankar A, Hunter J, Tufik S, Yu FH, Catterall WA, Mantegazza M, Goldin AL, Escayg A (2009) A BAC transgenic mouse model reveals neuron subtype-specific effects of a generalized epilepsy with febrile seizures plus (GEFS+) mutation. *Neurobiol Dis* 35:91–102.
- Ullal GR, Satishchandra P, Shankar SK (1996) Hyperthermic seizures: an animal model for hot-water epilepsy. *Seizure* 5:221–228.
- Wu J, Javedan SP, Ellsworth K, Smith K, Fisher RS (2001) Gamma oscillation underlies hyperthermia-induced epileptiform-like spikes in immature rat hippocampal slices. *BMC Neurosci* 2:18.
- Yanagihara K, Mizuuchi K (2002) Mismatch-targeted transposition of Mu: a new strategy to map genetic polymorphism. *Proc Natl Acad Sci U S A* 99:11317–11321.
- Yu FH, Mantegazza M, Westenbroek RE, Robbins CA, Kalume F, Burton KA, Spain WJ, McKnight GS, Scheuer T, Catterall WA (2006) Reduced sodium current in GABAergic interneurons in a mouse model of severe myoclonic epilepsy in infancy. *Nat Neurosci* 9:1142–1149.